Emerging Chalcogenide based van der Waals Heterostructures for Ultrathin Excitonic Solar Cells with enhanced Photo-conversion Efficiency

Ponnappa Kechanda Prasanna and Sudip Chakraborty*

Materials Theory for Energy Scavenging (MATES Lab), Harish-Chandra Research Institute, A CI of Homi Bhabha National Institute, Chhatnag Road, Jhunsi, Prayagraj - 211019

E-mail: sudipchakraborty@hri.res.in,sudiphys@gmail.com

Different possible heterostructure stacking order

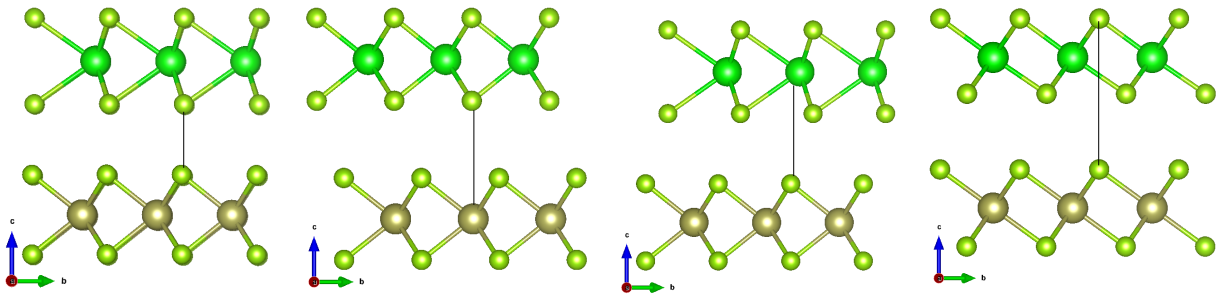

(a) AA stacking (b) AB stacking (c) AB′ stacking (d) AB″ stacking

Figure 1: Different stacking arrangements considered for structural optimization of hetero-bilayer.

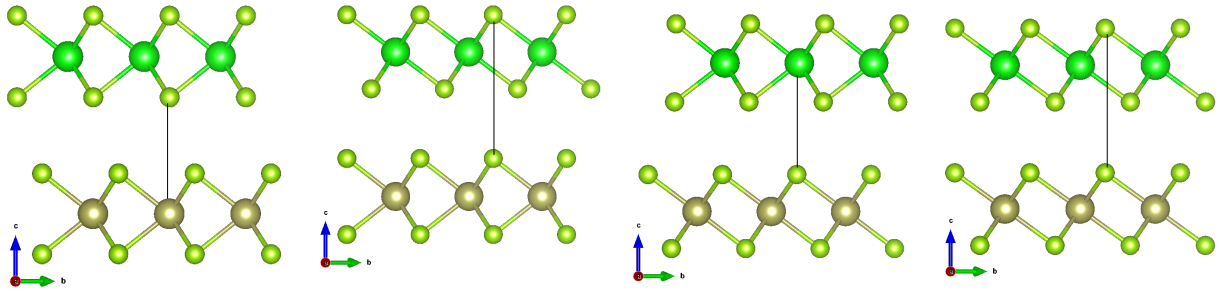

(a) $ZrSe_2$:2H/$HfSe_2$:2H (b) $ZrSe_2$:1T/$HfSe_2$:2H (c) $ZrSe_2$:2H/$HfSe_2$:1T (d) $ZrSe_2$:1T/$HfSe_2$:1T

Figure 2: Optimized geometry of hetero-bilayers with combination of different monolayers .

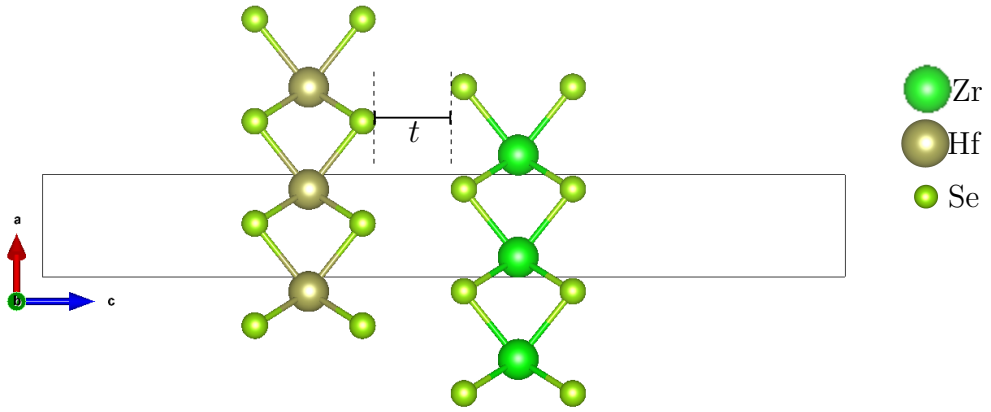

Figure 3: Schematic representation along the ac direction of hetero-bilayer (3×3 supercell), t is the distance between the layers.

Mechanical Stability

Monolayers

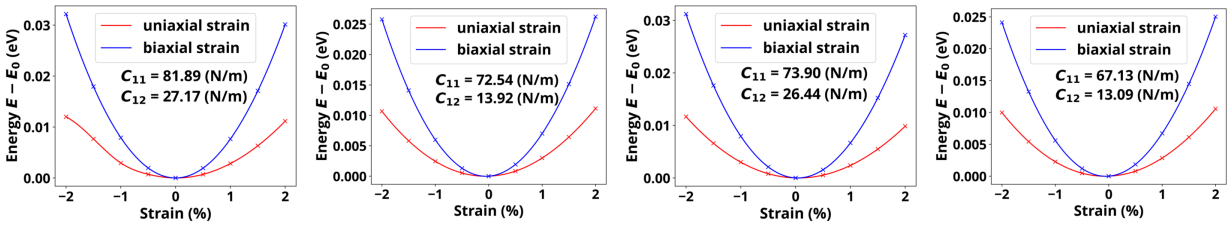

(a) $HfSe_2$:2H (b) $HfSe_2$:1T (c) $ZrSe_2$:2H (d) $ZrSe_2$:1T

Figure 4: Total energy variation for monolayers with applied external strain. C_{11} and C_{12} are the elastic constants. The blue line shows the variation of total energy with biaxial strain, while the red line shows that of the uni-axial strain.

Heterostructure

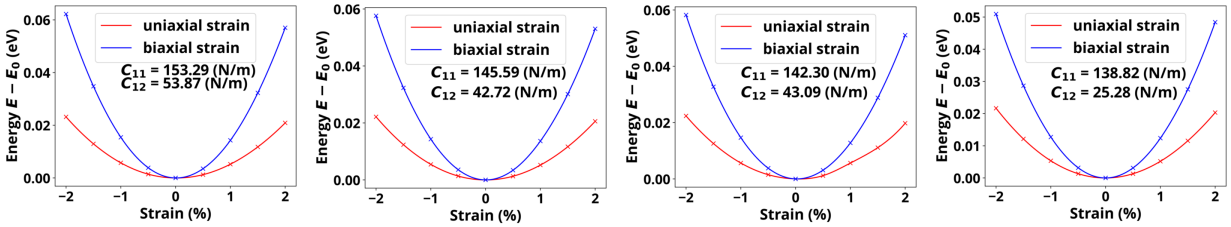

(a) $ZrSe_2$:2H/$HfSe_2$:2H (b) $ZrSe_2$:1T/$HfSe_2$:2H (c) $ZrSe_2$:2H/$HfSe_2$:1T (d) $ZrSe_2$:1T/$HfSe_2$:1T

Figure 5: Total energy variation for hetero-bilayer with applied external strain. C_{11} and C_{12} are the elastic constants. The blue line shows the variation of total energy with biaxial strain, while the red line shows that of the uni-axial strain.

Electronic Properties

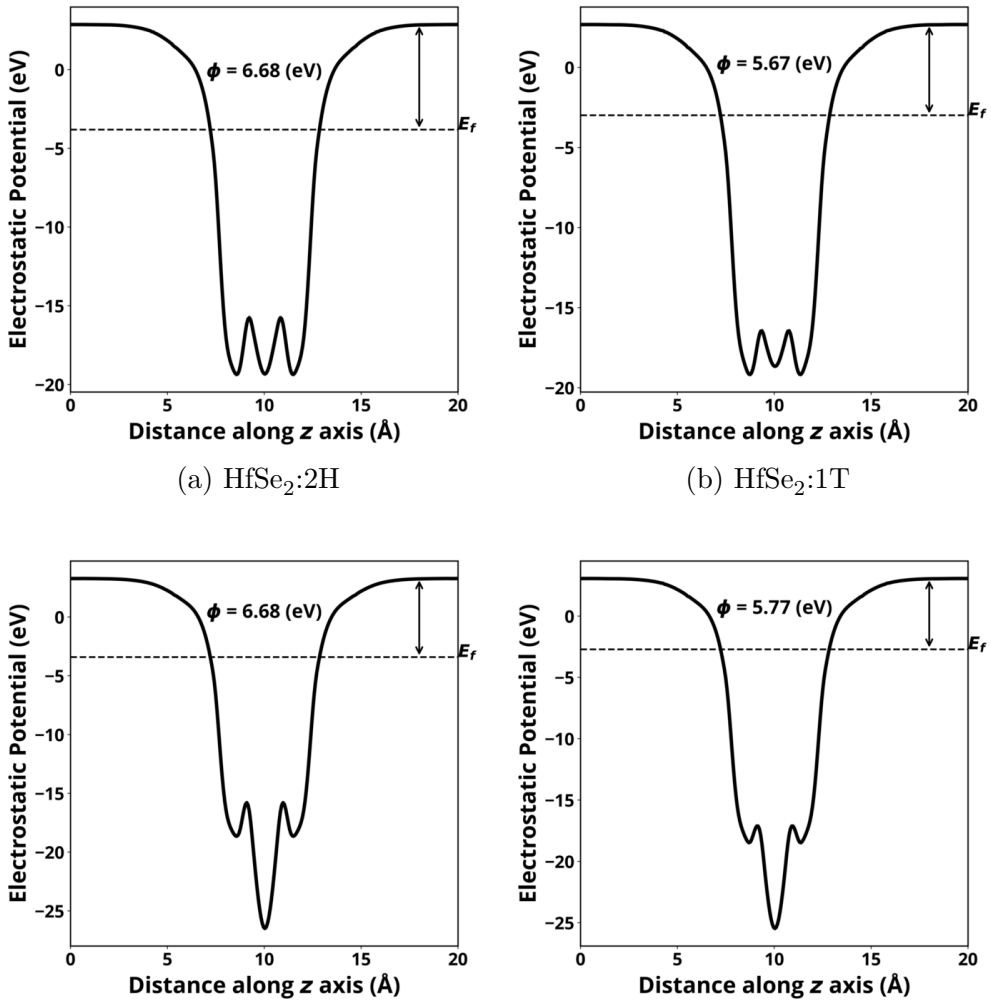

(a) $HfSe_2$:2H (b) $HfSe_2$:1T

(c) $ZrSe_2$:2H (d) $ZrSe_2$:1T

Figure 6: Electrostatic potential average along the z axis and the work function.

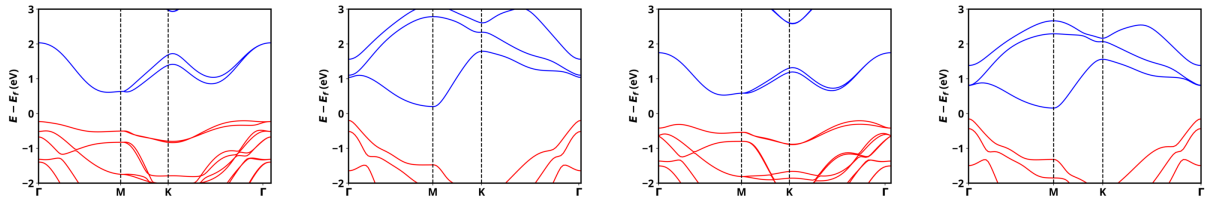

(a) $HfSe_2$:2H (b) $HfSe_2$:1T (c) $ZrSe_2$:2H (d) $ZrSe_2$:1T

Figure 7: Band structure of monolayers calculated using PBE.

Table 1: Deformation Potential E_{ex} and E_{hx} electrons and holes; Effective mass m_{e1} and m_{e2} of electrons, m_{h1} and m_{h2} of holes along two directions; and mobility μ_e, μ_h of electrons and holes, respectively in heterostructure.

Heterostructure	E_{ex} (eV)	E_{hx} (eV)	m^*_{e1} (m_0)	m^*_{e2} (m_0)	m^*_{h1} (m_0)	m^*_{h2} (m_0)	μ_e ($cm^2V^{-1}s^{-1}$)	μ_h ($cm^2V^{-1}s^{-1}$)
$ZrSe_2$:2H/$HfSe_2$:2H	-3.60	-3.26	1.07	2.43	-1.11	-2.23	146.00	175.90
$ZrSe_2$:1T/$HfSe_2$:2H	-7.16	-6.50	0.83	1.60	-0.16	-0.17	63.23	2781.22
$ZrSe_2$:1T/$HfSe_2$:1T	-2.89	-8.73	0.25	1.84	-0.16	-0.17	1859.70	1469.80

$ZrSe_2$:2H/$HfSe_2$:1T has a very low band gap and shows a metallic behaviour for PBE calculation therefore finding deformation potential for the same is not feasible.

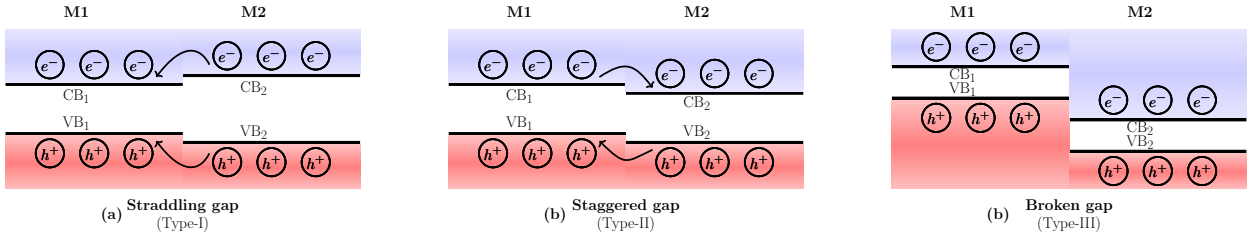

Figure 8: Three different possibilities of band alignment in semiconductor heterojunctions